Orbital degeneracy, Hund's coupling, and band ferromagnetism: Effective quantum parameter, suppression of quantum corrections, and enhanced stability

Bhaskar Kamble and Avinash Singh*
Department of Physics, Indian Institute of Technology, Kanpur 208016, India
(Received 5 May 2008; revised manuscript received 12 January 2009; published 11 February 2009)

An effective quantum parameter is obtained for the band ferromagnet in terms of orbital degeneracy and Hund's coupling. This quantum parameter determines, in analogy with $1/\mathcal{N}$ for the generalized Hubbard model and $1/S$ for quantum spin systems, the strength of quantum corrections to spin stiffness and spin-wave energies. Quantum corrections are obtained by incorporating correlation effects in the form of self-energy and vertex corrections within a spin-rotationally-symmetric approach in which the Goldstone mode is explicitly preserved order by order. It is shown that even a relatively small Hund's coupling is rather efficient in strongly suppressing quantum corrections, especially for large $\mathcal{N}$, resulting in strongly enhanced stability of the ferromagnetic state. This mechanism for the enhancement of ferromagnetism by Hund's coupling implicitly involves a subtle interplay of lattice, dimensionality, band dispersion, spectral distribution, and band filling effects.

DOI: 10.1103/PhysRevB.79.064410 PACS number(s): 75.30.Ds, 71.27.+a, 75.10.Lp, 71.10.Fd

I. INTRODUCTION

Experimental studies of magnetic and electronic excitations in various band ferromagnetic systems continue to be of strong current interest, as evidenced by intensive neutron-scattering studies of spin-wave excitations throughout the Brillouin zone in ferromagnetic manganites highlighting magnon damping and anomalous zone-boundary softening,[1] angle-resolved photoemission spectroscopy (ARPES) studies of iron to investigate many-body interaction between quasiparticles at the Fermi level,[2,3] and spin-polarized electron-energy-loss spectroscopy (SPEELS) studies of surface spin waves in ultrathin Fe films showing strong spin-wave softening due to reduction in exchange interaction.[4] Driven by recent advances in the resolution of experimental probes, these studies provide valuable insight into details of the microscopic mechanism and characteristics of band ferromagnetism.

Realistic multiband calculations of spin-wave dispersion using an itinerant-electron model, in bulk bcc Fe, e.g., have so far been carried out only in the random-phase approximation (RPA) owing to the complexity of the band structure.[5,6] Recently, a tight-binding model involving nine orbitals ($4s$, $4p$, and $3d$) per Fe atom has been used to calculate spin-wave dispersion in the RPA,[7] and electron self-energy corrections in the ferromagnetic phase of iron were studied in light of recent ARPES experiments on Fe.

Band ferromagnetism is in general an intermediate to strong coupling phenomenon.[8] Spin-wave excitations in a single-band ferromagnet are therefore strongly renormalized by correlation effects, as studied recently by incorporating self-energy and vertex corrections within a systematic inverse-degeneracy $(1/\mathcal{N})$ expansion scheme in which the spin-rotation symmetry of the Hamiltonian and hence the Goldstone mode[9] are explicitly preserved order by order beyond the RPA.[10] For the single-band Hubbard model, the correlation-induced minority-spin spectral-weight transfer was shown to result in strong spin-wave energy renormalization (quantum correction), and the interplay of lattice, band dispersion, and band filling effects was studied on the competition between the delocalization and exchange energy contributions to the spin stiffness, which fundamentally determines the stability of the ferromagnetic state in an itinerant ferromagnet.[11]

So how are quantum corrections generally affected by orbital multiplicity and Hund's coupling? This question is of fundamental importance in view of the multiband nature of transition-metal ferromagnets but has not been addressed so far in the literature. The special case of the $\mathcal{N}$-orbital Hubbard model with interaction $-(U/\mathcal{N})\Sigma_i(\Sigma_\mu \mathbf{S}_{i\mu})\cdot(\Sigma_\nu \mathbf{S}_{i\nu})$, where the indices μ,ν refer to the $\mathcal{N}$ degenerate orbitals at each lattice site i, has been considered earlier.[10] In this orbitally symmetric case, the interorbital interaction (Hund's coupling) is identical to the intraorbital interaction, and quantum corrections are simply suppressed by the inverse-degeneracy factor $1/\mathcal{N}$. However, for arbitrary Hund's coupling, the role of orbital degeneracy on quantum corrections to spin-wave excitations has not been investigated so far.

In this paper, we will extend the above Goldstone-mode-preserving approach for the study of correlation-induced quantum corrections to a multiband ferromagnet with arbitrary Hund's coupling. We will show that orbital multiplicity and Hund's coupling strongly suppress the quantum corrections and spin-wave energy renormalization in a band ferromagnet. We will further show the existence of an effective quantum parameter which, in analogy with $1/S$ for quantum spin systems and $1/\mathcal{N}$ for the orbitally symmetric $\mathcal{N}$-orbital Hubbard model, plays the role of $\hbar$ in effectively determining the magnitude of quantum corrections in a multiband ferromagnet.

A variety of methods have been employed to investigate the role of orbital degeneracy and Hund's coupling on the stability of metallic ferromagnetism, as briefly reviewed below. The magnetic phase diagram was obtained by finite-temperature quantum Monte Carlo calculations within the dynamical mean-field theory (DMFT).[12] While DMFT calculations for the single-orbital Hubbard model on fcc-type lattices showed that a necessary condition for ferromagnetism

was a highly asymmetric density of states (DOS) with large spectral weight near one of the band edges,[13] orbital degeneracy and finite Hund's coupling were shown to effectively stabilize ferromagnetism in a broad range of electron fillings even for a featureless DOS symmetric about the band center.[12]

Finite-temperature magnetism of iron and nickel was investigated using the LDA+DMFT (where LDA stands for local-density approximation) approach which combines DMFT with realistic electronic structure methods, and many-body features of the one-electron spectra and the observed magnetic moments were described.[14] The Coulomb interaction energy values used were $U=2.3(3.0)$ eV for Fe (Ni) and $J=0.9$ eV for both Fe and Ni, obtained from constrained LDA calculations.

The roles of lattice structure and Hund's coupling were investigated for various three-dimensional lattice structures within the DMFT using an improved quantum Monte Carlo algorithm that preserves the spin-SU(2) symmetry. It was shown that the earlier Ising-type DMFT calculations[12] overestimate the tendencies toward ferromagnetic ordering and the Curie temperature. Both the lattice structure and orbital degeneracy were found to be essential for the ferromagnetism in the parameter region representing a transition metal.[15,16] Other numerical techniques such as exact diagonalization,[17,18] density-matrix renormalization group,[19] slave boson,[20,21] and the Gutzwiller variational scheme[22] have also been employed.

The special case of two orbitals per site and quarter filling yields an insulating ferromagnetic state with staggered orbital ordering, as suggested by the equivalence to an "antiferromagnetic" state in the pseudospin space of the two orbitals, and first proposed as a mechanism for stabilization of ferromagnetism by Roth.[23] However, the estimated Curie temperature was found to be too low for transition-metal ferromagnets by a factor of 10. The insulating ferromagnetic state at quarter filling has also been investigated at strong coupling[24,25] and using the exact diagonalization method.[26–28]

II. TWO-ORBITAL HUBBARD MODEL WITH HUND'S COUPLING

We consider a degenerate two-orbital Hubbard model,

$$H = -\sum_{\langle ij\rangle,\sigma} t_{ij}(a^{\dagger}_{i\sigma\alpha}a_{j\sigma\alpha} + a^{\dagger}_{i\sigma\beta}a_{j\sigma\beta} + \text{H.c.}) - U\sum_{i}(\mathbf{S}_{i\alpha}\cdot\mathbf{S}_{i\alpha} + \mathbf{S}_{i\beta}\cdot\mathbf{S}_{i\beta}) - 2J\sum_{i}(\mathbf{S}_{i\alpha}\cdot\mathbf{S}_{i\beta}), \quad (1)$$

where α and β refer to the two degenerate orbitals at each lattice site i and $\mathbf{S}_{i\mu}=\psi^{\dagger}_{i\mu}(\boldsymbol{\sigma}/2)\psi_{i\mu}$ are the local spin operators for the two orbitals $\mu=\alpha,\beta$ in terms of the fermionic operators $\psi^{\dagger}_{i\mu}=(a^{\dagger}_{i\uparrow\mu}a^{\dagger}_{i\downarrow\mu})$ and the Pauli matrices $\boldsymbol{\sigma}$. The hopping terms $t_{ij}=t$ for nearest neighbors and t' for next-nearest neighbors. The above model includes an intraorbital Hubbard interaction U and an interorbital Hund's coupling J. As our objective is to investigate the role of Hund's coupling on quantum corrections in the orbitally degenerate ferromagnetic state, we have not retained the interorbital density-density interaction term $V_0 n_{i\alpha}n_{i\beta}$, also conventionally included in the orbital Hubbard model. This density interaction term is important in the context of orbital ordering in manganites,[24] especially near quarter filling,[23] as expected from its structural similarity with an antiparallel-spin interaction in the pseudospin (α,β) space, which will favor antiferromagnetic orbital ordering.

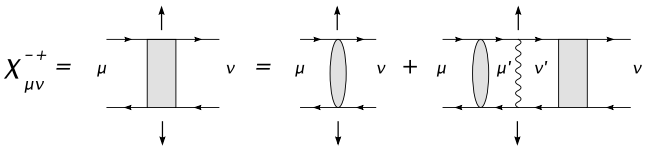

FIG. 1. Exact diagrammatic representation of the transverse spin propagator in terms of the irreducible particle-hole propagator.

The orbital Hubbard model above has been written in an explicitly spin-rotationally-symmetric form. This continuous symmetry implies the existence of Goldstone modes in the spontaneously-broken-symmetry state,[9] which will play a central role in our study of correlation effects in the ferromagnetic state in which self-energy and vertex corrections are systematically incorporated such that the Goldstone mode is explicitly preserved order by order.

III. TRANSVERSE SPIN FLUCTUATIONS

We assume a ferromagnetic ground state with polarization in the z direction and examine transverse spin fluctuations representing both collective spin-wave and single-particle Stoner excitations. We consider the time-ordered transverse spin-fluctuation propagator in this broken-symmetry state:

$$\chi^{-+}_{\mu\nu}(\mathbf{q},\omega) = i\int dt e^{i\omega(t-t')}\sum_{j} e^{i\mathbf{q}\cdot(\mathbf{r}_i-\mathbf{r}_j)}\langle\Psi_0|\mathrm{T}[S^{-}_{i\mu}(t)S^{+}_{j\nu}(t')]|\Psi_0\rangle, \quad (2)$$

where the orbital indices $\mu,\nu=\alpha,\beta$ and the fermion spin-lowering and spin-raising operators $S^{\mp}_{i\mu}=\psi^{\dagger}_{i\mu}(\sigma^{\mp}/2)\psi_{i\mu}$.

The transverse spin-fluctuation propagators can be expressed exactly in terms of the irreducible particle-hole propagators ϕ, as shown diagrammatically in Fig. 1. The corresponding coupled equations are

$$\chi^{-+}_{\mu\nu}(\mathbf{q},\omega) = \phi_{\mu\nu}(\mathbf{q},\omega) + \phi_{\mu\mu'}(\mathbf{q},\omega)U_{\mu'\nu'}\chi^{-+}_{\nu'\nu}(\mathbf{q},\omega), \quad (3)$$

where the interaction term $U_{\mu'\nu'}=U$ for $\mu'=\nu'$ and $U_{\mu'\nu'}=J$ for $\mu'\neq\nu'$ is shown as the wavy line in Fig. 1, and summation over repeated indices is implied.

As external probes such as magnetic field or the neutron magnetic moment couple equally to electron magnetic moments in the two degenerate orbitals, it is physically relevant to consider the sum

$$\chi^{-+}(\mathbf{q},\omega) = \chi^{-+}_{\alpha\alpha}(\mathbf{q},\omega) + \chi^{-+}_{\alpha\beta}(\mathbf{q},\omega) \quad (4)$$

of the intraorbital and interorbital contributions. Indeed, it is particularly convenient to solve the coupled equations for the total transverse propagator, and we obtain

$$\chi^{-+}(\mathbf{q},\omega) = \frac{\phi(\mathbf{q},\omega)}{1-(U+J)\phi(\mathbf{q},\omega)}, \tag{5}$$

where

$$\phi(\mathbf{q},\omega) = \phi_{\alpha\alpha}(\mathbf{q},\omega) + \phi_{\alpha\beta}(\mathbf{q},\omega) \tag{6}$$

represents the total irreducible particle-hole propagator, for which a systematic expansion will be discussed below.

IV. SYSTEMATIC EXPANSION FOR THE IRREDUCIBLE PARTICLE-HOLE PROPAGATOR ϕ

In analogy with the inverse-degeneracy $(1/\mathcal{N})$ expansion for the orbitally symmetric $\mathcal{N}$-orbital Hubbard model,[10] we consider a systematic expansion:

$$\phi = \phi^{(0)} + \phi^{(1)} + \phi^{(2)} + \ldots \tag{7}$$

for the irreducible propagator $\phi(\mathbf{q},\omega)$ in orders of fluctuations. The first term $\phi^{(0)}$ is simply the bare particle-hole propagator, whereas the higher-order terms $\phi^{(1)}, \phi^{(2)}$, etc., represent quantum corrections involving self-energy and vertex corrections, as discussed below.

In the inverse-degeneracy expansion scheme,[10] the diagrams were systematized in terms of the expansion parameter $1/\mathcal{N}$, with the nth-order term $\phi^{(n)}$ involving n powers of $1/\mathcal{N}$. Thus the expansion parameter $1/\mathcal{N}$ played, in analogy with $1/S$ for quantum spin systems, the role of $\hbar$. In the following we will show that the dimensionless factor $(U^2+J^2)/(U+J)^2$ (and a similar factor for the $\mathcal{N}$ orbital case) plays the role of the expansion parameter for arbitrary Hund's coupling. This allows for a continuous interpolation between the orbitally independent limit $(J=0)$ and the orbitally symmetric limit $(J=U)$.

A. Random-phase approximation

Retaining only the zeroth-order term $\phi^{(0)}$ yields the RPA, amounting to a "classical" description of noninteracting spin-fluctuation modes. As the hopping term is diagonal in orbital indices, the zeroth-order term involves only the intraorbital contribution:

$$\phi^{(0)}_{\alpha\alpha}(\mathbf{q},\omega) \equiv \chi_0(\mathbf{q},\omega) = \sum_{\mathbf{k}} \frac{1}{\epsilon^{\downarrow +}_{\mathbf{k}-\mathbf{q}} - \epsilon^{\uparrow -}_{\mathbf{k}} + \omega - i\eta}, \tag{8}$$

where the Hartree-Fock level band energies $\epsilon^{\sigma}_{\mathbf{k}} = \epsilon_{\mathbf{k}} - \sigma\Delta$ involve the exchange splitting,

$$2\Delta = (U+J)m, \tag{9}$$

between the two spin bands. The superscripts $+(-)$ refer to particle (hole) states above (below) the Fermi energy ϵ_F. Here the magnetization $\mathbf{m} = 2\langle \mathbf{S}_{i\mu}\rangle$ is assumed to be identical for both orbitals $\mu = \alpha, \beta$ in the orbitally degenerate ferromagnetic state. For the saturated ferromagnet, the magnetization m is equal to the particle density n for each orbital.

At the RPA level, the two (intraorbital and interorbital) components of the transverse spin propagator are easily obtained by solving the coupled Eq. (3), and we obtain

$$[\chi^{-+}_{\alpha\alpha}(\mathbf{q},\omega)]_{\mathrm{RPA}} = \frac{1}{2}\left[\frac{\chi_0(\mathbf{q},\omega)}{1-U^+\chi_0(\mathbf{q},\omega)} + \frac{\chi_0(\mathbf{q},\omega)}{1-U^-\chi_0(\mathbf{q},\omega)}\right] = [\chi^{-+}_{\beta\beta}(\mathbf{q},\omega)]_{\mathrm{RPA}}, \tag{10}$$

$$[\chi^{-+}_{\alpha\beta}(\mathbf{q},\omega)]_{\mathrm{RPA}} = \frac{1}{2}\left[\frac{\chi_0(\mathbf{q},\omega)}{1-U^+\chi_0(\mathbf{q},\omega)} - \frac{\chi_0(\mathbf{q},\omega)}{1-U^-\chi_0(\mathbf{q},\omega)}\right] = [\chi^{-+}_{\beta\alpha}(\mathbf{q},\omega)]_{\mathrm{RPA}}, \tag{11}$$

where the two effective interaction terms above are $U^{\pm} = U \pm J$. As seen, the propagators involve linear combinations of in-phase and out-of-phase modes with respect to orbitals. These two modes represent gapless (acoustic) and gapped (optical) branches, as shown below. We also introduce kernels for these two propagators which will be used later in the expressions for quantum corrections:

$$[\Gamma^{-+}_{\alpha\alpha}]_{\mathrm{RPA}} = ([\chi^{-+}_{\alpha\alpha}]_{\mathrm{RPA}} - \chi_0)/\chi_0^2 = \frac{1}{2}\left[\frac{U^+}{1-U^+\chi_0} + \frac{U^-}{1-U^-\chi_0}\right], \tag{12}$$

$$[\Gamma^{-+}_{\alpha\beta}]_{\mathrm{RPA}} = [\chi^{-+}_{\alpha\beta}]_{\mathrm{RPA}}/\chi_0^2 = \frac{1}{2}\left[\frac{U^+}{1-U^+\chi_0} - \frac{U^-}{1-U^-\chi_0}\right]. \tag{13}$$

The in-phase mode with effective interaction $U^+ = U+J$ corresponds to the usual Goldstone mode (acoustic branch). This is expected as the exchange splitting $2\Delta = (U+J)m$ in the χ_0 energy denominator involves the same effective interaction U^+. On the other hand, the out-of-phase mode with effective interaction $U^- = U-J$ yields gapped excitations (optical branch). A typical spectral function plot is shown in Fig. 3, with the inset showing dispersion of the acoustic and optical branches and onset of Stoner excitations.

From Eqs. (5) and (8), poles of the magnon propagator yield the (gapless) magnon energies $\omega^0_{\mathbf{q}}$ at the RPA level. The spin stiffness $D = \omega_{\mathbf{q}}/q^2$, defined in terms of the magnon energy for small $\mathbf{q}$, provides a quantitative measure of the stability of the ferromagnetic state against long-wavelength fluctuations, with negative D signaling loss of long-range magnetic order. We briefly review the different contributions to spin stiffness at the RPA level as their behavior and interplay provide insight into the magnitude of the first-order quantum corrections and of ferromagnetic-state stability, as discussed in Sec. IV B.

Expanding $\chi_0(\mathbf{q},\omega)$ given in Eq. (8) for small $\mathbf{q},\omega$, the bare (RPA) spin stiffness can be expressed as[10]

$$D^{(0)} = \frac{1}{d}\left[\frac{1}{2}\langle \nabla^2 \epsilon_{\mathbf{k}}\rangle - \frac{\langle (\nabla \epsilon_{\mathbf{k}})^2\rangle}{2\Delta}\right] \tag{14}$$

in d dimensions. Here the angular bracket $\langle\ \rangle$ represents momentum summation normalized over the number of occupied states $(\frac{1}{m}\Sigma_{\mathbf{k}})$. The two terms in Eq. (14) of order t and t^2/U^+ represent hopping and exchange contributions to the spin stiffness, respectively, corresponding to delocalization-energy loss and exchange-energy gain upon spin twisting. The stability of the ferromagnetic state therefore involves a subtle competition between the hopping contribution which

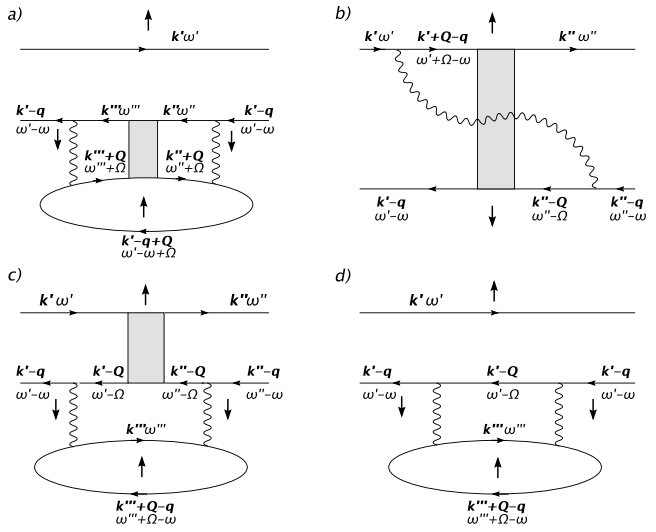

FIG. 2. The first-order quantum corrections to the irreducible particle-hole propagator.

favors the FM state and the exchange contribution which tends to destabilize it. Both the hopping and exchange contributions are sensitive to lattice structure, band dispersion, and band filling.[11]

B. Quantum corrections

In the following we consider first-order quantum corrections to the irreducible particle-hole propagator [Eq. (7)]. We consider the relatively simpler case of a saturated ferromagnet in which the minority-spin particle-hole processes are absent as the minority-spin band is pushed above the Fermi energy due to Coulomb repulsion. In this case the effective antiparallel-spin interactions at lowest order reduce to the bare interactions U and J, and the effective parallel-spin interactions reduce to a single term involving the majority-spin particle-hole bubble. Generally, these effective interactions involve a series of bubble diagrams, with even and odd numbers of bubbles, respectively.

Diagrammatic contributions to the first-order quantum correction $\phi^{(1)}$ are shown in Fig. 2. The interaction lines are either U or J, depending on the orbitals of the connecting fermion lines. The external ($\mu=\alpha,\beta$ on the right) orbital degrees of freedom are also summed over to include both the intraorbital and interorbital contributions as in Eq. (6). The physical meaning of the four diagrams has been discussed earlier.[10] Diagrams (a) and (d) represent corrections to the irreducible propagator due to self-energy corrections to the spin-$\downarrow$ particle arising from spin and charge fluctuations, respectively. The shaded part in diagram (a) represents the propagator $\chi^{-+}_{\mathrm{RPA}}(\mathbf{Q},\Omega)$. Diagrams (b) and (c) represent vertex corrections, where the shaded part represents the kernel $\Gamma^{-+}_{\mathrm{RPA}}(\mathbf{Q},\Omega)$ introduced in Eqs. (12) and (13). In diagram (b), the opposite-spin *particle-particle* interaction suppresses the spin-$\downarrow$ particle–spin-$\uparrow$ hole correlation, yielding a negative correction to ϕ. Diagram (b) therefore represents suppression of the magnetic response due to particle-particle correlations. All four diagrams involve a spin-charge coupling, as indicated by the spin-$\uparrow$ particle-hole bubble present explicitly in diagrams (c) and (d) and implicitly in (a) and (b).

Integrating out the fermion frequency-momentum degrees of freedom, the first-order quantum corrections to the irreducible particle-hole propagator are obtained as

$$\phi^{(a)}(\mathbf{q},\omega)=\sum_{\mathbf{Q}}\int\frac{d\Omega}{2\pi i}\{(U^2+J^2)\chi^{-+}_{\alpha\alpha}(\mathbf{Q},\Omega)+2UJ\chi^{-+}_{\alpha\beta}(\mathbf{Q},\Omega)\}\times\sum_{\mathbf{k}'}\left(\frac{1}{\epsilon^{\downarrow+}_{\mathbf{k}'-\mathbf{q}}-\epsilon^{\uparrow-}_{\mathbf{k}'}+\omega-i\eta}\right)^2\times\left(\frac{1}{\epsilon^{\uparrow+}_{\mathbf{k}'-\mathbf{q}+\mathbf{Q}}-\epsilon^{\uparrow-}_{\mathbf{k}'}+\omega-\Omega-i\eta}\right),\tag{15}$$

$$\phi^{(b)}(\mathbf{q},\omega)=-2\sum_{\mathbf{Q}}\int\frac{d\Omega}{2\pi i}\{U\Gamma^{-+}_{\alpha\alpha}(\mathbf{Q},\Omega)+J\Gamma^{-+}_{\alpha\beta}(\mathbf{Q},\Omega)\}\times\sum_{\mathbf{k}'}\left(\frac{1}{\epsilon^{\downarrow+}_{\mathbf{k}'-\mathbf{q}}-\epsilon^{\uparrow-}_{\mathbf{k}'}+\omega-i\eta}\right)\times\left(\frac{1}{\epsilon^{\uparrow+}_{\mathbf{k}'-\mathbf{q}+\mathbf{Q}}-\epsilon^{\uparrow-}_{\mathbf{k}'}+\omega-\Omega-i\eta}\right)\times\sum_{\mathbf{k}''}\left(\frac{1}{\epsilon^{\downarrow+}_{\mathbf{k}''-\mathbf{Q}}-\epsilon^{\uparrow-}_{\mathbf{k}''}+\Omega-i\eta}\right)\times\left(\frac{1}{\epsilon^{\downarrow+}_{\mathbf{k}''-\mathbf{q}}-\epsilon^{\uparrow-}_{\mathbf{k}''}+\omega-i\eta}\right),\tag{16}$$

$$\phi^{(c)}(\mathbf{q},\omega)=\sum_{\mathbf{Q}}\int\frac{d\Omega}{2\pi i}\{(U^2+J^2)\Gamma^{-+}_{\alpha\alpha}(\mathbf{Q},\Omega)+2UJ\Gamma^{-+}_{\alpha\beta}(\mathbf{Q},\Omega)\}\times\left[\sum_{\mathbf{k}'}\left(\frac{1}{\epsilon^{\downarrow+}_{\mathbf{k}'-\mathbf{q}}-\epsilon^{\uparrow-}_{\mathbf{k}'}+\omega-i\eta}\right)\times\left(\frac{1}{\epsilon^{\downarrow+}_{\mathbf{k}'-\mathbf{Q}}-\epsilon^{\uparrow-}_{\mathbf{k}'}+\Omega-i\eta}\right)\right]^2\times\sum_{\mathbf{k}''}\left(\frac{1}{\epsilon^{\uparrow+}_{\mathbf{k}''-\mathbf{q}+\mathbf{Q}}-\epsilon^{\uparrow-}_{\mathbf{k}''}+\omega-\Omega-i\eta}\right),\tag{17}$$

$$\phi^{(d)}(\mathbf{q},\omega)=\sum_{\mathbf{Q}}\int\frac{d\Omega}{2\pi i}(U^2+J^2)\sum_{\mathbf{k}'}\left(\frac{1}{\epsilon^{\downarrow+}_{\mathbf{k}'-\mathbf{q}}-\epsilon^{\uparrow-}_{\mathbf{k}'}+\omega-i\eta}\right)^2\times\left(\frac{1}{\epsilon^{\downarrow+}_{\mathbf{k}'-\mathbf{Q}}-\epsilon^{\uparrow-}_{\mathbf{k}'}+\Omega-i\eta}\right)\times\sum_{\mathbf{k}''}\left(\frac{1}{\epsilon^{\uparrow+}_{\mathbf{k}''-\mathbf{q}+\mathbf{Q}}-\epsilon^{\uparrow-}_{\mathbf{k}''}+\omega-\Omega-i\eta}\right).\tag{18}$$

The χ^{-+} and Γ^{-+} appearing above are at the RPA level but could be replaced by the renormalized propagators within a self-consistent theory. We note that in the $J\to 0$ limit of decoupled orbitals, we recover the single-band Hubbard model results.[10]

As collective spin-wave excitations are represented by poles in Eq. (5), spin-rotation symmetry requires that $\phi = 1/(U+J)$ for $q,\omega=0$, corresponding to the Goldstone mode. Since the zeroth-order term $\phi^{(0)}$ already exhausts this requirement, the sum of the remaining terms must exactly vanish in order to preserve the Goldstone mode. For this cancellation to hold for arbitrary J and U, each higher-order term $\phi^{(n)}$ in expansion (7) must individually vanish, implying that spin-rotation symmetry is preserved order by order. This cancellation is demonstrated below for the first-order quantum correction.

Towards this end, we note that the boson term (quantity in braces) in Eq. (16) for $\phi^{(b)}$ can be expressed as

$$U\Gamma^{-+}_{\alpha\alpha} + J\Gamma^{-+}_{\alpha\beta} = \{(U^2+J^2)\chi^{-+}_{\alpha\alpha} + 2UJ\chi^{-+}_{\alpha\beta}\}/\chi_0, \tag{19}$$

which is of identical form as the boson terms in Eqs. (15) and (17) for $\phi^{(a)}$ and $\phi^{(c)}$. With $\epsilon^{\downarrow+}_{\mathbf{k}-\mathbf{q}} - \epsilon^{\uparrow-}_{\mathbf{k}} = 2\Delta$ for $q=0$, we obtain, from Eqs. (15)–(18),

$$\begin{aligned}
\phi^{(1)}(q=0,\omega) &= \phi^{(a)} + \phi^{(b)} + \phi^{(c)} + \phi^{(d)} \\
&= \sum_{\mathbf{Q}} \int \frac{d\Omega}{2\pi i} \left(\frac{1}{2\Delta + \omega - i\eta} \right)^2 \\
&\times \sum_{\mathbf{k}'} \left(\frac{1}{\epsilon^{\uparrow+}_{\mathbf{k}'+\mathbf{Q}} - \epsilon^{\uparrow-}_{\mathbf{k}'} + \omega - \Omega - i\eta} \right) \\
&\times [\{(U^2+J^2)\chi^{-+}_{\alpha\alpha} + 2UJ\chi^{-+}_{\alpha\beta}\} \\
&- 2\{(U^2+J^2)\chi^{-+}_{\alpha\alpha} + 2UJ\chi^{-+}_{\alpha\beta}\} \\
&+ \{(U^2+J^2)(\chi^{-+}_{\alpha\alpha} - \chi_0) + 2UJ\chi^{-+}_{\alpha\beta}\} \\
&+ \{(U^2+J^2)\chi_0\}],
\end{aligned} \tag{20}$$

which yields identically vanishing contribution for each spin-fluctuation mode $\mathbf{Q}$, thus preserving the Goldstone mode. We note that this mode-by-mode cancellation is quite independent of the spectral-weight distribution of the spin-fluctuation spectrum between collective spin-wave and particle-hole Stoner excitations. Furthermore, the cancellation holds for all ω, indicating no spin-wave amplitude renormalization, as expected for the saturated ferromagnet in which there are no quantum corrections to magnetization.

Evaluation of the Ω integral in Eqs. (15)–(18) has been discussed earlier.[11] Using a spectral representation it is convenient to carry out the Ω integral numerically so as to include all three (acoustic, optical, and Stoner) contributions from the magnon (χ^{-+},Γ^{-+}) and the particle-hole terms. A typical spectral function plot of the RPA-level magnon propagator shows (Fig. 3) the low-energy (acoustic), intermediate-energy (optical), and high-energy (Stoner) contributions, with the inset showing the dispersion of acoustic and optical branches and onset energy of the Stoner branch. Here and in the following, all energies have been expressed in units of the hopping term t.

V. HUND'S COUPLING AND SUPPRESSION OF QUANTUM CORRECTIONS

We will now show that Hund's coupling results in a strong suppression of quantum corrections, and this is the central message of this paper. The suppression is approximately by an overall factor of $(U^2+J^2)/(U+J)^2$ for the two orbital case and by a factor of $[U^2+(\mathcal{N}-1)J^2]/[U+(\mathcal{N}-1)J]^2$ for the $\mathcal{N}$ orbital case. The magnitude of the overall factor is asymptotically exact in the two limits $J\to 0$ and $J\to U$. In these two limits the factor approaches 1 and 1/2, respectively, for the two orbital case, whereas it approaches 1 and $1/\mathcal{N}$, respectively, for the $\mathcal{N}$ orbital case. Indeed, for our degenerate two-orbital Hubbard model [Eq. (1)], this overall factor plays the same role as $1/\mathcal{N}$ in the orbitally symmetric $\mathcal{N}$-orbital Hubbard model[10] and generalizes this earlier result to the case of arbitrary Hund's coupling. In the orbitally symmetric case, the interaction term $-U(\Sigma_\mu \mathbf{S}_{i\mu})(\Sigma_\nu \mathbf{S}_{i\nu})$ involves identical interorbital and intraorbital interactions $(J=U)$.

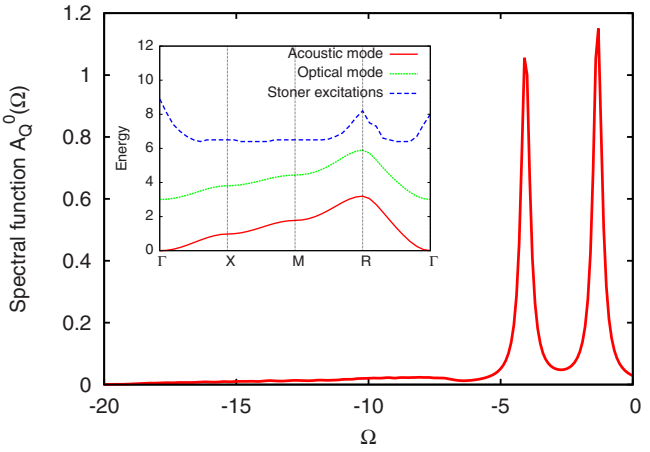

FIG. 3. (Color online) All three contributions—the low-energy (acoustic), intermediate-energy (optical), and high-energy (Stoner)—as seen in a typical spectral function plot of the magnon propagator $[\chi^{-+}_{\alpha\alpha}(\mathbf{Q},\Omega)]_{\mathrm{RPA}}$ for $\mathbf{Q}=(\frac{\pi}{2},\frac{\pi}{2},\frac{\pi}{2})$, are included in evaluating the Ω integral in Eqs. (15)–(18). Inset shows the dispersion of the acoustic and optical branches and the onset energy for the Stoner branch for the sc lattice with $t'=0.25$, $U=15$, $J=3$, and band filling $n=0.5$.

To see this overall suppression factor, we consider Eqs. (15)–(18) for the quantum corrections ϕ. In Eq. (15), assuming similar contributions from the acoustic and optical modes, which is a good approximation in the $J \ll U$ limit when the two modes become nearly degenerate, the boson term $2UJ\chi^{-+}_{\alpha\beta}$ yields negligible contribution in view of the opposite contributions [Eq. (11)] of the acoustic and optical modes. Hence, only the contribution from the first boson term $(U^2+J^2)\chi^{-+}_{\alpha\alpha}$ survives, leaving an overall factor (U^2+J^2) on carrying out the $\mathbf{Q},\Omega$ integration. Comparing with the corresponding factor $(U+J)^2$ for the equivalent single-orbital case (with identical exchange splitting) yields an overall relative factor of $(U^2+J^2)/(U+J)^2$. In view of Eq. (19), the quantum correction $\phi^{(b)}$ also involves the same boson term and hence yields the same overall factor. Similarly, the quantum corrections $\phi^{(c)}$ and $\phi^{(d)}$ together yield the same boson term and hence the same overall factor.

Extending to $\mathcal{N}$ orbitals, the first boson term in Eq. (15) will be $[U^2+(\mathcal{N}-1)J^2]\chi^{-+}_{\alpha\alpha}$, where U^2 corresponds to an intraorbital scattering (α to α) at each of the two interaction vertices shown, and J^2 corresponds to the $(\mathcal{N}-1)$ interorbital

scatterings (α to β), which yield identical contributions as $\chi^{-+}_{\alpha\alpha}=\chi^{-+}_{\beta\beta}$ in the orbitally degeneracy ferromagnetic state. The contribution of the other boson term in Eq. (15) involving the interorbital magnon propagator $\chi^{-+}_{\alpha\beta}$ will continue to be small. Again, comparing with the corresponding factor $[U+(\mathcal{N}-1)J]^2$ for the equivalent single-orbital case yields an overall relative factor of $[U^2+(\mathcal{N}-1)J^2]/[U+(\mathcal{N}-1)J]^2$.

The magnitude of the overall factor is also exact in the $J\to U$ limit, as shown below. The boson term in Eq. (15) can be identically written, in view of Eqs. (10) and (11), as

$$(U^2+J^2)\chi^{-+}_{\alpha\alpha}+2UJ\chi^{-+}_{\alpha\beta}=\frac{1}{2}[(U+J)^2\chi^{-+}_{\mathrm{aco}}+(U-J)^2\chi^{-+}_{\mathrm{opt}}], \tag{21}$$

in terms of the acoustic and optical branches. Therefore, in the $J\to U$ limit, the contribution of the optical mode vanishes, leaving an overall factor of 1/2, as also resulting from the expression $(U^2+J^2)/(U+J)^2$.

The topology of the first-order diagrams shown in Fig. 2 (for arbitrary J) is exactly the same as that for the $J=U$ case.[10] This will hold to all orders due to the similarity of the two models. Higher-order diagrams will therefore involve multiples of the same diagrammatic elements. For example, diagrams at the second order can have two self-energy insertions as in (a) or one self-energy insertion (a) and one crossed ladder (b), etc. As these elements yield the same factor $(U^2+J^2)/(U+J)^2$, the nth-order diagrams will involve n powers of this factor.

Band ferromagnetism being a strong-coupling phenomenon, quantum corrections to spin stiffness and magnon energy for the single-orbital Hubbard model with $U\sim W$ have been shown to yield strong renormalizations (reduction relative to the RPA values) in two and three dimensions.[11] The strong suppression of quantum corrections shown above highlights the critical role of Hund's coupling in stabilizing ferromagnetism in realistic systems such as transition metals Fe, Ni, and Co with multiple $3d$ orbitals. We propose that in such systems, Hund's coupling favors ferromagnetism by strongly suppressing the quantum corrections.

VI. QUANTUM CORRECTIONS TO SPIN STIFFNESS

We now consider the net quantum correction ϕ for small q in order to obtain the renormalized spin stiffness, which provides a quantitative measure of the stability of the ferromagnetic state with respect to long-wavelength fluctuations. In Eqs. (15)–(18), writing the antiparallel-spin particle-hole energy denominator as

$$\epsilon^{\downarrow+}_{\mathbf{k}-\mathbf{q}}-\epsilon^{\uparrow-}_{\mathbf{k}}=2\Delta[1+(\epsilon_{\mathbf{k}-\mathbf{q}}-\epsilon_{\mathbf{k}})/2\Delta] \tag{22}$$

and expanding in powers of the small band-energy difference,

$$\delta\equiv-(\epsilon_{\mathbf{k}-\mathbf{q}}-\epsilon_{\mathbf{k}})=\mathbf{q}\cdot\boldsymbol{\nabla}\epsilon_{\mathbf{k}}-\frac{1}{2}(\mathbf{q}\cdot\boldsymbol{\nabla})^2\epsilon_{\mathbf{k}}, \tag{23}$$

we find that besides the zeroth-order cancellation for $q=0$, the first-order terms in δ also exactly cancel. This exact cancellation implies that there is no quantum correction to the delocalization contribution $\langle\boldsymbol{\nabla}^2\epsilon_{\mathbf{k}}\rangle$ in the spin-stiffness constant; only the exchange contribution in the spin stiffness is renormalized by the surviving second-order terms in δ, and we obtain for the first-order quantum correction to stiffness:

$$\begin{aligned}D^{(1)}=2\Delta(U+J)\phi^{(1)}/q^2=\frac{1}{d}\frac{(U+J)}{(2\Delta)^3}\sum_{\mathbf{Q}}\int\frac{d\Omega}{2\pi i}&\times\Bigg[U^a_{\mathrm{eff}}(\mathbf{Q},\Omega)\Bigg(\sum_{\mathbf{k}'}\frac{(\boldsymbol{\nabla}\epsilon_{\mathbf{k}'})^2}{\epsilon^{\uparrow+}_{\mathbf{k}'+\mathbf{Q}}-\epsilon^{\uparrow-}_{\mathbf{k}'}-\Omega-i\eta}\Bigg)\\&-\frac{2U^a_{\mathrm{eff}}(\mathbf{Q},\Omega)}{\chi^0(\mathbf{Q},\Omega)}\Bigg(\sum_{\mathbf{k}'}\frac{\boldsymbol{\nabla}\epsilon_{\mathbf{k}'}}{\epsilon^{\uparrow+}_{\mathbf{k}'+\mathbf{Q}}-\epsilon^{\uparrow-}_{\mathbf{k}'}-\Omega-i\eta}\Bigg)\\&\times\Bigg(\sum_{\mathbf{k}''}\frac{\boldsymbol{\nabla}\epsilon_{\mathbf{k}''}}{\epsilon^{\downarrow+}_{\mathbf{k}''-\mathbf{Q}}-\epsilon^{\uparrow-}_{\mathbf{k}''}+\Omega-i\eta}\Bigg)\\&+\frac{U^c_{\mathrm{eff}}(\mathbf{Q},\Omega)}{\chi^2_0(\mathbf{Q},\Omega)}\Bigg(\sum_{\mathbf{k}'}\frac{1}{\epsilon^{\uparrow+}_{\mathbf{k}'+\mathbf{Q}}-\epsilon^{\uparrow-}_{\mathbf{k}'}-\Omega-i\eta}\Bigg)\\&\times\Bigg(\sum_{\mathbf{k}''}\frac{\boldsymbol{\nabla}\epsilon_{\mathbf{k}''}}{\epsilon^{\downarrow+}_{\mathbf{k}''-\mathbf{Q}}-\epsilon^{\uparrow-}_{\mathbf{k}''}+\Omega-i\eta}\Bigg)^2\\&+(U^2+J^2)\Bigg(\sum_{\mathbf{k}''}\frac{1}{\epsilon^{\uparrow+}_{\mathbf{k}'+\mathbf{Q}}-\epsilon^{\uparrow-}_{\mathbf{k}'}-\Omega-i\eta}\Bigg)\\&\times\Bigg(\sum_{\mathbf{k}''}\frac{(\boldsymbol{\nabla}\epsilon_{\mathbf{k}''})^2}{\epsilon^{\downarrow+}_{\mathbf{k}''-\mathbf{Q}}-\epsilon^{\uparrow-}_{\mathbf{k}''}+\Omega-i\eta}\Bigg)\Bigg],\end{aligned} \tag{24}$$

where d is the lattice dimensionality. Here we have introduced effective interactions in the transverse channel:

$$U^a_{\mathrm{eff}}=\{(U^2+J^2)\chi^{-+}_{\alpha\alpha}(\mathbf{Q},\Omega)+2UJ\chi^{-+}_{\alpha\beta}\},$$

$$U^c_{\mathrm{eff}}=U^a_{\mathrm{eff}}-(U^2+J^2)\chi^0. \tag{25}$$

As $\boldsymbol{\nabla}\epsilon_{\mathbf{k}}$ is odd in momentum, the second and third terms in Eq. (23) give vanishingly small contributions due to partial cancellation.

The behavior of quantum correction to spin stiffness with band filling is shown in Fig. 4 for different values of the Hund's coupling J. Here we have kept $U+J$ fixed so that the exchange band splitting and the classical spin stiffness remain unchanged. The quantum correction to spin stiffness decreases sharply with J and reduces to exactly half the magnitude when $J=U$, as shown in Fig. 5 for two different band fillings. Inset shows a comparison of the normalized quantum correction calculated from Eq. (23) with the approximate form $[1+(J/U)^2]/[1+J/U]^2$, which asymptotically approaches the calculated result in the two limits $J/U\to 0$ and $J/U\to 1$, as discussed in Sec. V. These results clearly show that even a small Hund's coupling is rather efficient in strongly suppressing the quantum correction.

We now discuss the behavior of the renormalized spin stiffness, which is obtained from the magnon energy $\omega_{\mathbf{q}}=2\Delta[1-U^+\phi(\mathbf{q})]=Dq^2$ for small q, where $\phi=\phi^{(0)}+\phi^{(1)}$ includes the quantum correction up to first order. From the contributions $U^+\phi^{(0)}=1-D^{(0)}q^2/2\Delta$ [Eq. (8)] and $U^+\phi^{(1)}$

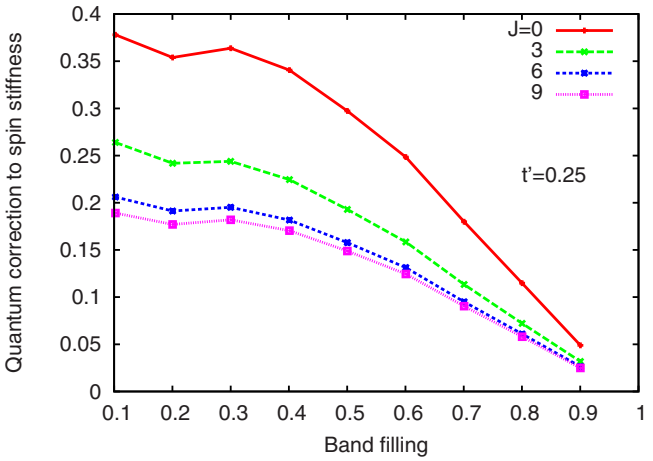

FIG. 4. (Color online) Quantum correction to spin stiffness for the simple cubic lattice shown as a function of band filling for different J with fixed $U+J=1.5W=18t$.

$=D^{(1)}q^2/2\Delta$ [Eq. (24)] of the classical and quantum terms, we obtain the renormalized spin stiffness $D=D^{(0)}-D^{(1)}$. Physically, the quantum correction $D^{(1)}$ corresponds to a correlation-induced exchange contribution (of order t^2/U^+) to spin stiffness,[10,11] which together with the (negative) classical exchange contribution in Eq. (14), further reduces the spin stiffness.

Figure 6 shows that the renormalized spin stiffness D rapidly changes sign from negative to positive with increasing J, highlighting the effective stabilization of ferromagnetism by Hund's coupling, shown here for the simple cubic (sc) lattice with $t'=0.25$ and fixed $U+J=1.5W$.

As discussed in Sec. V, generalizing to the $\mathcal{N}$-orbital case, the spin-stiffness quantum correction should be approximately suppressed by the factor $[U^2+(\mathcal{N}-1)J^2]/[U+(\mathcal{N}-1)J]^2$. With increasing Hund's coupling, this factor rapidly approaches $1/\mathcal{N}$, particularly for large $\mathcal{N}$; the orbitally symmetric $\mathcal{N}$-orbital Hubbard model therefore provides a good

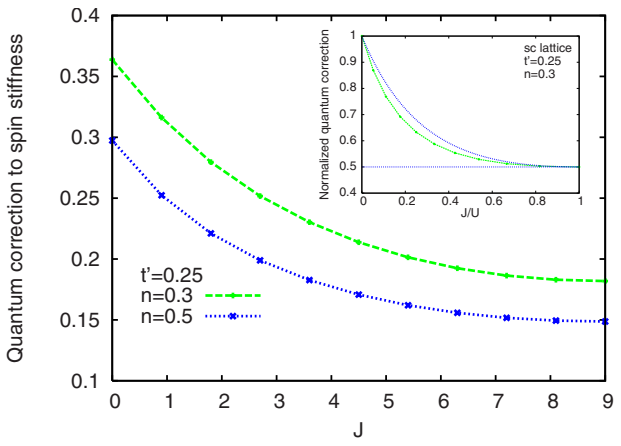

FIG. 5. (Color online) Rapid suppression of quantum correction to spin stiffness with Hund's coupling J shown for the sc lattice at two different band fillings. Inset shows comparison of the normalized quantum correction with the approximate form $[1+(J/U)^2]/(1+J/U)^2$, which asymptotically approaches the calculated result in the two limits $J/U\to 0$ and $J/U\to 1$.

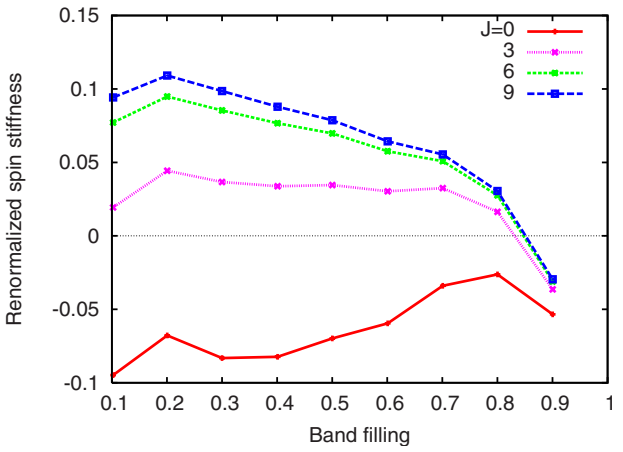

FIG. 6. (Color online) The effective stabilization of the ferromagnetic state by Hund's coupling is shown by the rapid change in J from negative to positive spin stiffness, shown as a function of band filling for the simple cubic lattice with $t'=0.25$ and fixed $U+J=1.5W$.

approximation for transition-metal ferromagnets with five $3d$ orbitals.

We have examined the role of this $1/\mathcal{N}$ suppression of quantum correction on the spin stiffness for the orbitally symmetric $\mathcal{N}$-orbital Hubbard model (with $J=U$). In this case the renormalized spin stiffness can be expressed as $D=D^{(0)}-\frac{1}{\mathcal{N}}D^{(1)}_{\mathcal{N}=1}$ with the quantum correction suppression factor $1/\mathcal{N}$ explicitly pulled out, where $D^{(1)}_{\mathcal{N}=1}$ represents the correction for the single-orbital case. Figure 7 shows the renormalized spin stiffness for different number of orbitals $\mathcal{N}$, evaluated for a bcc lattice with $t'/t=0.5$, bandwidth $W=16t=3.2$ eV, Coulomb interaction energy $U=W=3.2$ eV, and the lattice parameter $a=2.87$ Å for Fe.

In a recent band-structure calculation for Fe,[7] the interaction energy considered is $U=2.13$ eV (so that the magnetic moment evaluated per Fe atom is equal to $2.12\mu_B$) and the bandwidth from the calculated DOS plot is seen to be about

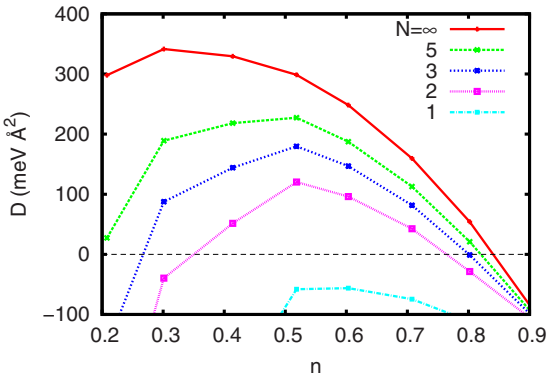

FIG. 7. (Color online) Renormalized spin stiffness for the generalized $\mathcal{N}$-orbital Hubbard model (with $J=U$) for different number of orbitals $\mathcal{N}$, showing the $1/\mathcal{N}$ suppression of quantum corrections with orbital degeneracy, evaluated for the bcc lattice with bandwidth $W=16t=3.2$ eV, Coulomb interaction energy $U=W=3.2$ eV, and lattice parameter $a=2.87$ Å for Fe. The measured value for Fe is 280 meV Å^2.

4 eV. The calculated electronic density of states shows the majority band to be nearly filled and the minority band nearly half filled. Within a particle-hole transformation, this corresponds to a nearly saturated ferromagnet with a nearly half-filled ($n \sim 0.5$) lower band and a nearly empty upper band. Our calculated values for the renormalized spin stiffness for $\mathcal{N}=5$ at the corresponding band filling ($n \sim 0.5$) are close to the measured value 280 meV Å^2 for Fe. The spin stiffness is seen to involve a quantum reduction in about 25% near optimal filling.

VII. RENORMALIZED MAGNON DISPERSION

Turning now to the magnon dispersion over the entire Brillouin zone, the renormalized magnon energy $\omega_{\mathbf{q}}$ for finite $\mathbf{q}$ is obtained from the pole condition $1-(U+J)\mathrm{Re}\,\phi(\mathbf{q},-\omega_{\mathbf{q}})=0$ in Eq. (5), where $\phi(\mathbf{q},\omega)=\phi^{(0)}(\mathbf{q},\omega)+\phi^{(1)}(\mathbf{q},\omega)$, and the four contributions to the first-order quantum correction $\phi^{(1)}(\mathbf{q},\omega)$ are given in Eqs. (15)–(18). While the bare particle-hole propagator $\phi^{(0)}(\mathbf{q},\omega)$ remains real in the relevant ω range, the quantum correction $\phi^{(1)}(\mathbf{q},\omega)$ is complex for any finite $\omega<0$ due to the coupling with charge fluctuations, resulting in finite zero-temperature magnon damping.[29] Both collective and Stoner excitations are included in evaluating the Ω integral, as discussed below Eq. (20).

The effect of Hund's coupling on the renormalized magnon dispersion is shown in Figs. 8 and 9, which provide comparisons of the bare ($\omega_{\mathbf{q}}^0$) and renormalized ($\omega_{\mathbf{q}}$) magnon dispersions along symmetry directions for the simple cubic and square lattices, respectively. Again $U+J$ was kept fixed so that the bare magnon energy remains unchanged. While Hund's coupling increases the magnon energy in the entire Brillouin zone, the effect is particularly dramatic for long-wavelength modes, which rapidly crossover from negative-energy to positive-energy modes.

Even when the bare magnon dispersion exhibits nearly Heisenberg form, with energies at X,M,R approximately in the ratio 1:2:3 as in Fig. 8(b), the renormalized magnon dispersion shows strong anomalous softening at X relative to R. This indicates that magnon renormalization due to spin-charge coupling results in the "generation" of additional exchange couplings J_2,J_3,J_4, etc., within an equivalent localized-spin model with the same magnon dispersion.

The renormalized spin stiffness and magnon energies obtained above essentially determine the finite-temperature spin dynamics and therefore the Curie temperature T_c. Due to spin-flip scattering of electrons accompanying thermal magnon excitation, a portion of the majority-spin spectral weight is transferred to the minority-spin band above the Fermi energy, while an equal amount of minority-spin spectral weight is transferred to the majority-spin band below the Fermi energy. A finite-temperature analysis of this spectral weight transfer across the Fermi energy, the resulting magnetization reduction, and Curie temperature for the Hubbard model have been discussed in Ref. 11 within a renormalized spin-fluctuation theory in which the magnon amplitude and energy are self-consistently renormalized by the factor $\langle S_z\rangle_T/\langle S_z\rangle_0$, which ensures that the sum rule $\langle[S^+,S^-]\rangle = \langle 2S_z\rangle$ is obeyed.

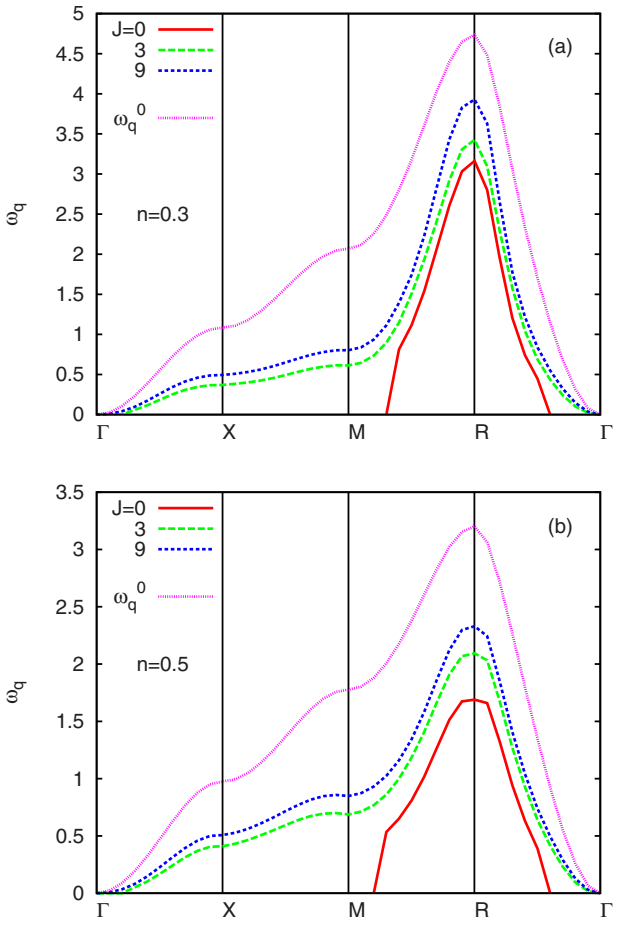

FIG. 8. (Color online) Hund's coupling results in a strongly momentum-dependent enhancement of magnon energies as seen from the magnon dispersion along symmetry directions in the Brillouin zone for the sc lattice at two different band fillings with $t'=0.25$ and fixed $U+J=18t=1.5W$. The rapid crossover from negative-energy to positive-energy long-wavelength modes with J shows the strong stabilization of ferromagnetism by Hund's coupling.

Extending the above analysis for finite Hund's coupling, the electron-magnon interaction term is modified to $(U^2+J^2)\chi^{-+}_{\alpha\alpha}+2UJ\chi^{-+}_{\alpha\beta}$ as in Eq. (15), which can be written as $(1/2)[(U+J)^2\chi^{-+}_{\mathrm{aco}}+(U-J)^2\chi^{-+}_{\mathrm{opt}}]$ using the resolution of the transverse spin propagators [Eqs. (10) and (11)] into acoustic and optical modes. If $\omega_{\mathbf{q}}$ and $\omega^*_{\mathbf{q}}$ refer to the magnon energies of the acoustic and optical modes, assuming similar magnon amplitude and energy renormalizations within the spin-fluctuation theory,[11] the Curie temperature is approximately obtained as

$$\frac{1}{k_B T_c} \approx \frac{1}{2}\left[(U+J)^2\sum_{\mathbf{q}}\frac{2}{\omega_{\mathbf{q}}}+(U-J)^2\sum_{\mathbf{q}}\frac{2}{\omega^*_{\mathbf{q}}}\right] \times\sum_{\mathbf{k}}\left(\frac{1}{\epsilon^{\downarrow+}_{\mathbf{k}-\mathbf{q}}-\epsilon^{\uparrow-}_{\mathbf{k}}}\right)^2. \tag{26}$$

Now, finite Hund's coupling results in (i) gapped optical modes with higher energies ($\omega^*_{\mathbf{q}}>\omega_{\mathbf{q}}$) than the acoustic modes, (ii) reduced weight of the optical modes due to the

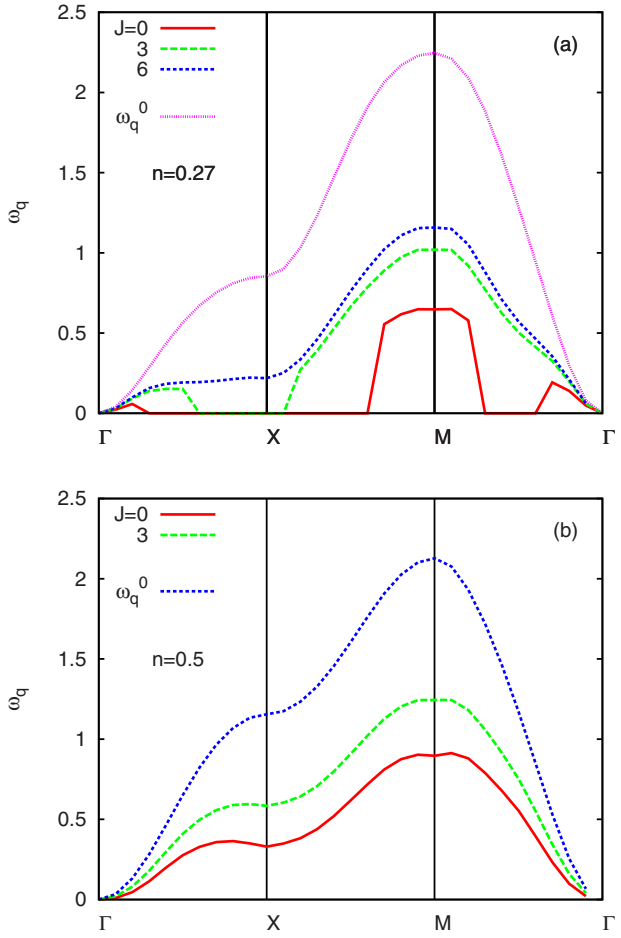

FIG. 9. (Color online) Rapid suppression of quantum correction and stabilization of ferromagnetism due to Hund's coupling as seen in the magnon dispersion along symmetry directions for the square lattice at two different band fillings with $t'=0.5$ and fixed $U+J=12t=1.5W$. The dispersion along the Γ-X direction shows pronounced anomalous softening near the zone boundary.

$(U-J)^2$ factor in above equation, and (iii) enhancement of the acoustic magnon-mode energies (even at fixed $U+J$). All three factors suppress the right-hand side of above equation, directly resulting in enhanced Curie temperature. While this enhancement of T_c is in general agreement with DMFT studies where only local excitations are incorporated, Eq. (26) highlights the sensitivity to long-wavelength modes as well in our Goldstone-mode-preserving approach. Negative-energy long-wavelength modes as in Figs. 8 and 9 would result in vanishing T_c even if bulk of the (short-wavelength) modes have positive energy. Long-wavelength modes play a particularly important role in low-dimensional systems. The divergence of the right-hand side of Eq. (26) in one and two dimensions yields vanishing T_c in accordance with the Mermin-Wagner theorem.[30]

We now qualitatively discuss the effects of the interorbital Coulomb interaction term. Being an extension of our earlier Hubbard-model analysis, the diagrams considered in Fig. 2 actually correspond to a density interaction term $\Sigma_{\sigma,\sigma'}(V_0-J\delta_{\sigma\sigma'})n_{\alpha\sigma}n_{\beta\sigma'}$, with $V_0=J$, involving only opposite-spin interactions.

The remaining interorbital interaction term is therefore $(V_0-J)\Sigma_{\sigma,\sigma'}n_{\alpha\sigma}n_{\beta\sigma'}$. Being a density interaction, it contributes neither to the exchange splitting nor to the spin-fluctuation propagator $[\chi^{-+}]_{\mathrm{RPA}}$ involving only ladder diagrams with transverse interaction terms S^-S^+ etc. Therefore, the spin-stiffness quantum correction from diagram (a) in Fig. 2 involving self-energy correction due to spin fluctuations remains unchanged. The enhancement of ferromagnetism due to suppression of quantum corrections by orbital degeneracy and Hund's coupling is therefore an independent feature.

However, the density interaction (V_0-J) does contribute to additional spin-stiffness quantum corrections arising from interorbital density fluctuations (diagrams similar to (d) involving self-energy correction due to bubble diagrams with alternating α and β orbitals and only spin-$\uparrow$ bubbles as minority-spin particle-hole processes are absent in the saturated ferromagnet). This first-order self-energy correction physically incorporates the correlation effect of suppressed simultaneous occupancy of the two orbitals.

This additional density-fluctuation contribution will involve the charge fluctuation propagator $\chi_0/[1-(V_0-J)\chi_0][1+(V_0-J)\chi_0]$. Therefore, in the vicinity of the orbital-ordering transition $[(V_0-J)\chi_0\sim 1]$, the strong interorbital density fluctuations will yield significant spin-stiffness quantum reduction and render the orbitally degenerate ferromagnet unstable. A complete account of this transition will require investigating quantum effects on spin stiffness in the orbitally ordered ferromagnetic state as well.

Far away from the orbital-ordering instability $[(V_0-J)\chi_0 \ll 1]$, implicitly assumed in the orbitally degenerate ferromagnetic state considered here, these additional quantum corrections will be relatively insignificant.

VIII. CONCLUSIONS

The role of orbital degeneracy and Hund's coupling on quantum corrections to spin-wave excitations in a band ferromagnet was investigated. A spin-rotationally-symmetric approach was employed in which self-energy and vertex corrections are incorporated systematically so that the Goldstone mode is explicitly preserved order by order. The present study of quantum corrections for arbitrary Hund's coupling allows for a continuous interpolation between the orbitally independent case $(J=0)$ equivalent to the single-band Hubbard model and the orbitally symmetric case of identical interorbital and intraorbital Coulomb interactions $(J=U)$, for which the first-order quantum corrections are suppressed by the factor $1/\mathcal{N}$. We find that even a relatively small Hund's coupling is rather efficient in strongly suppressing the quantum corrections, especially for large $\mathcal{N}$, resulting in a strong enhancement of ferromagnetism.

This mechanism for the enhancement of ferromagnetism by Hund's coupling implicitly involves an interplay of several band and lattice characteristics. Competition between the delocalization $\langle\nabla^2\epsilon_{\mathbf{k}}\rangle$ and exchange $\langle(\nabla\epsilon_{\mathbf{k}})^2\rangle/2\Delta$ contributions to spin-stiffness results in a subtle interplay of lattice, dimensionality, band dispersion, spectral distribution, Coulomb interaction, and band filling effects, as investigated for

several two-dimensional and three-dimensional lattices.[11]

For a two-orbital Hubbard model, the first-order quantum correction to spin stiffness was obtained diagrammatically and evaluated as a function of the Hund's coupling strength J. We showed that the effective quantum correction factor decreases rapidly from 1 at $J=0$ to 1/2 at $J=U$, and its behavior with J closely follows the approximate form $(U^2+J^2)/(U+J)^2$ obtained from our diagrammatic analysis. In the intermediate-coupling regime, with interaction strength U comparable to the bandwidth, the renormalized spin stiffness was evaluated in the whole range of band fillings and was found to rapidly crossover from negative to positive values with increasing Hund's coupling, highlighting the strong role of orbital degeneracy and Hund's coupling on the stability of the ferromagnetic state with respect to long-wavelength fluctuations. We also obtained, for both the square and simple cubic lattices, the renormalized spin-wave energy dispersion $\omega_{\mathbf{q}}$ for momenta along symmetry directions in the Brillouin zone. While Hund's coupling results in an enhancement of the magnon energy in the entire Brillouin zone, the effect is particularly dramatic for long-wavelength modes, which rapidly crossover from negative to positive energy.

Generalizing to the $\mathcal{N}$ orbital case, an effective quantum parameter $[U^2+(\mathcal{N}-1)J^2]/[U+(\mathcal{N}-1)J]^2$ was obtained which, in analogy with $1/S$ for quantum spin systems and $1/\mathcal{N}$ for the orbitally symmetric Hubbard model, plays the role of $\hbar$ for quantum corrections in a band ferromagnet. For large $\mathcal{N}$, this quantum parameter decreases rapidly with the Hund's coupling J and saturates to $1/\mathcal{N}$ as $J \to U$.

Physically, the suppression of quantum corrections due to orbital degeneracy and Hund's coupling is because of inter-orbital incoherence of spin fluctuations ($\langle S^+_{i\alpha} S^-_{i\beta} \rangle = 0$). Therefore, the off-diagonal channels involving $\chi^{-+}_{\alpha\beta}$ do not contribute to the electron-magnon scattering, and the matrix-element square is reduced to $U^2+(\mathcal{N}-1)J^2$ as compared to $[U+(\mathcal{N}-1)J]^2$ for the equivalent single-orbital case. The spin-stiffness quantum correction is therefore reduced as it is basically an additional exchange-type contribution due to the spin-$\downarrow$ spectral redistribution resulting from the electron-magnon interaction.

This strong suppression of quantum corrections due to orbital degeneracy and Hund's coupling is quite significant for the $3d$ transition-metal ferromagnets Fe, Co, and Ni, where $\mathcal{N}=5$. With $J/U=1/4$, as considered in the recent RPA calculations for iron,[7] we obtain a value of $5/16 \approx 0.3$ for the quantum parameter. While the smallness of this quantum correction parameter accounts for why RPA calculations of the spin stiffness for Fe with realistic band structure yield values in close agreement with the measured value of 280 meV Å^2, it also highlights the significant magnitude of the correlation-induced quantum corrections involved in the measured spin-stiffness values for transition-metal ferromagnets.

*avinas@iitk.ac.in

[1] F. Ye, P. Dai, J. A. Fernandez-Baca, D. T. Adroja, T. G. Perring, Y. Tomioka, and Y. Tokura, Phys. Rev. B **75**, 144408 (2007).
[2] J. Schafer, M. Hoinkis, E. Rotenberg, P. Blaha, and R. Claessen, Phys. Rev. B **72**, 155115 (2005).
[3] X. Y. Cui, K. Shimada, M. Hoesch, Y. Sakisaka, H. Kato, Y. Aiura, M. Higashiguchi, Y. Miura, H. Namatame, and M. Taniguchi, Surf. Sci. **601**, 4010 (2007).
[4] W. X. Tang, Y. Zhang, I. Tudosa, J. Prokop, M. Etzkorn, and J. Kirschner, Phys. Rev. Lett. **99**, 087202 (2007).
[5] J. F. Cooke, J. W. Lynn, and H. L. Davis, Phys. Rev. B **21**, 4118 (1980).
[6] J. A. Blackman, T. Morgan, and J. F. Cooke, Phys. Rev. Lett. **55**, 2814 (1985).
[7] M. Naito and D. S. Hirashima, J. Phys. Soc. Jpn. **76**, 044703 (2007).
[8] D. Vollhardt, N. Blümer, K. Held, M. Kollar, J. Schlipf, M. Ulmke, and J. Wahle, Adv. Solid State Phys. **38**, 383 (1999).
[9] J. Goldstone, A. Salam, and S. Weinberg, Phys. Rev. **127**, 965 (1962).
[10] A. Singh, Phys. Rev. B **74**, 224437 (2006).
[11] S. Pandey and A. Singh, Phys. Rev. B **75**, 064412 (2007); **76**, 104437 (2007).
[12] K. Held and D. Vollhardt, Eur. Phys. J. B **5**, 473 (1998).
[13] M. Ulmke, Eur. Phys. J. B **1**, 301 (1998).
[14] A. I. Lichtenstein, M. I. Katsnelson, and G. Kotliar, Phys. Rev. Lett. **87**, 067205 (2001).
[15] S. Sakai, R. Arita, K. Held, and H. Aoki, Phys. Rev. B **74**, 155102 (2006).
[16] S. Sakai, R. Arita, and H. Aoki, arXiv:0706.3109 (unpublished).
[17] K. Kusakabe and H. Aoki, Physica B **194-196**, 217 (1994).
[18] T. Momoi and K. Kubo, Phys. Rev. B **58**, R567 (1998).
[19] H. Sakamoto, T. Momoi, and K. Kubo, Phys. Rev. B **65**, 224403 (2002).
[20] R. Fresard and G. Kotliar, Phys. Rev. B **56**, 12909 (1997).
[21] A. Klejnberg and J. Spalek, Phys. Rev. B **61**, 15542 (2000).
[22] J. Bünemann, W. Weber, and F. Gebhard, Phys. Rev. B **57**, 6896 (1998).
[23] L. M. Roth, Phys. Rev. **149**, 306 (1966).
[24] K. I. Kugel and D. I. Khomskii, Sov. Phys. JETP **37**, 725 (1973).
[25] M. Cyrot and C. Lyon-Caen, J. Phys. (Paris) **36**, 253 (1975); J. Phys. C **9**, 3789 (1976).
[26] W. Gill and D. J. Scalapino, Phys. Rev. B **35**, 215 (1987).
[27] J. E. Hirsch, Phys. Rev. B **56**, 11022 (1997).
[28] J. Kuei and R. T. Scalettar, Phys. Rev. B **55**, 14968 (1997).
[29] S. Pandey and A. Singh, Phys. Rev. B **78**, 014414 (2008).
[30] N. D. Mermin and H. Wagner, Phys. Rev. Lett. **17**, 1133 (1966).